

Contents lists available at ScienceDirect

Physics Letters B

www.elsevier.com/locate/physletb

Probing the top quark chromoelectric and chromomagnetic dipole moments in single top tW -channel at the LHC



Seyed Yaser Ayazi*, Hoda Hesari, Mojtaba Mohammadi Najafabadi

School of Particles and Accelerators, Institute for Research in Fundamental Sciences (IPM), P.O. Box 19395-5531, Tehran, Iran

ARTICLE INFO

Article history:

Received 28 July 2013

Received in revised form 17 September 2013

Accepted 9 October 2013

Available online 17 October 2013

Editor: J. Hisano

ABSTRACT

We study the effects of chromoelectric and chromomagnetic dipole moments (CEDM and CMDM) on the production cross section of single top tW -channel at the LHC based on the effective Lagrangian approach. We show that the impact of CEDM and CMDM could be large. Using the experimental measurement of the tW -channel cross section, constraints on CEDM and CMDM are extracted. These constraints are comparable with the ones obtained from the top pair analysis.

© 2013 Elsevier B.V. All rights reserved.

1. Introduction

The top quark is the heaviest Standard Model (SM) particle which has been discovered so far, and might be the first place in which new physics effects could appear. The top quark has been discovered and studied in some details at the Tevatron, many of its properties are being studied at the LHC with high precision.

Since new physics can show up in the couplings of the top quark with other SM particles, in particular with gauge bosons, the precise measurement of the top couplings with other SM fields is important. The LHC experiments are the places to probe these couplings because the top quark is copiously produced at the LHC [1].

At the LHC, top quarks are produced primarily via two independent mechanisms. The dominant production mechanism is the pair production processes $q\bar{q} \rightarrow t\bar{t}$, $g g \rightarrow t\bar{t}$ and the second is single top production via electroweak interactions involving the Wtb vertex. Single top quarks at the LHC are produced in three different modes: The s -channel (the involved W is time-like), the t -channel mode (the involved W is space-like), and the tW production (the W boson is real). Despite single top has a smaller cross section than top pair production, it can play an important role in studying of the top quark physics at the LHC because this channel has potential to allow a direct measurement of V_{tb} CKM matrix elements as well as its sensitivity to various new physics models. However sufficient integrated luminosity and improved method of analysis can help us achieve detection and precise measurement of single top at the LHC. The first observable in single top study is the total cross section and measurement of any possible deviation from the SM value. Therefore, it is worthwhile to investigate the effects of physics beyond SM on single top quark production.

The SM has been successfully able to describe most of experimental measurements with high precisions. Nevertheless, it is commonly accepted that it is a valid effective Lagrangian which is applicable at low energies. In many beyond SM theories which have been studied to date, reduction to the SM at low energies proceeds via decoupling of heavy particle with masses of order Λ . There have been many attempts to study the sensitivity of the LHC observables to various effective operators [2]. Our goal in this Letter is to study the effect of anomalous couplings of the top quark with gluon via tW -channel of single top at the LHC. We will assume that new physics effects in tW single top production are induced by consideration of an effective Lagrangian. Here, we confine our studies to interaction of mass dimension 5 after spontaneous symmetry breaking. The total statistical and systematic uncertainties in the measurement of cross section for this process at the LHC is about 25% with an integrated luminosity of 4.9 fb^{-1} [3]. The top quark is the heaviest quark, therefore effects of new physics on its coupling are expected to be larger than for any other fermions and deviation with respect to the SM values might be detectable.

The rest of this Letter is organized as follows: In the next section, considering the effective Lagrangian for $gt\bar{t}$ coupling, we calculate the analytical expression for the single tW top cross section production at the LHC. In Section 3, we present the dependency of observables which we study at the LHC. Then, we find the allowed regions in parameters space of our effective Lagrangian and compare our results with the results obtained from observables in production of $t\bar{t}$ at LHC and EDM of the top quark. The conclusions are given in Section 4.

2. Framework and analytical calculations

In this section, we introduce a model independent effective Lagrangian for the vertex of $gt\bar{t}$ and look for any possible deviation

* Corresponding author.

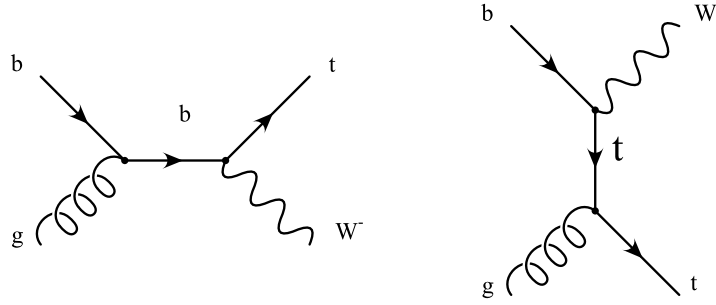


Fig. 1. Feynman diagrams for the tW -channel of single top.

from SM prediction in production of tW -channel at the LHC. In this approach, the SM is modified by an addition 5-dimensional Lagrangian which includes interaction of top pair and gluon and consider the effect of this Lagrangian in production of tW single top production. Coefficients of this Lagrangian parameterize the low energy effects of the underlying high scale physics. The gauge invariant effective Lagrangian for the interactions between the top quark and gluons which include the CEDM and CMDM form factors is given by:

$$\mathcal{L}_{eff} = g_s \bar{t} \lambda^a \gamma^\mu t G_\mu^a + g_s \bar{t} \lambda^a \frac{\sigma^{\mu\nu} q_\mu}{4m_t} [F_2(q^2) + i\gamma^5 F_3(q^2)] t G_\mu^a \quad (1)$$

where λ^a ($a = 1, \dots, 8$) are the $SU(3)_C$ color matrices and $F_2(q^2)$ and $F_3(q^2)$ are, respectively, the CMDM and CEDM form factors of the top quark. Notice that a sizable non-zero CEDM would be the signal of a new type of CP-violating interaction beyond CKM phase and can contribute to EDM of neutron. For this reason, experimental upper bound on EDM of neutron constraint this coupling [4–8]. The effects of top quark CEDM and CMDM on the top production at next linear colliders, on the decay of B-meson to $s\gamma$ have been studied in literature [9,10].

In the following, we use this constraint on parameters space of above Lagrangian and compare these bounds with our result which arise from tW single top production at LHC.

Assuming $|q^2| \ll \Lambda$, where Λ is the scale of new physics, the form factors can be approximated by

$$F_3(q^2) \approx \tilde{\kappa}, \quad F_2(q^2) \approx \kappa \quad \text{for } |q^2| \ll \Lambda \quad (2)$$

where $\tilde{\kappa}$ and κ are independent of q^2 . The CMDM of the top quark is then given by $\frac{g_s \kappa}{(2m_t)}$, while CEDM is $\frac{g_s \tilde{\kappa}}{(2m_t)}$.

As it is shown in Fig. 1, $gt\bar{t}$ effective Lagrangian can contribute to the right diagram in tW of single top production at the LHC. We calculate the amplitude of $bg \rightarrow tW$ process including CEDM and CMDM effects. This amplitude is given by:

$$\overline{|M|^2} = \frac{g^2 g_s^2}{192} |V_{tb}|^2 \left[\frac{f_1}{(m_t^2 - \hat{u})^2} + \frac{m_W^2 f_2}{\hat{s}(m_t^2 - \hat{u})^2 (m_t^2 - \hat{u} m_t)^2} + \frac{f_3}{\hat{s} m_t^2 (m_t^2 - \hat{u})^2 m_W^2} + \frac{32 m_W^4}{\hat{s} (m_t^2 - \hat{u})} + \frac{\tilde{\kappa}^2 f_4}{m_t^2 m_W^2} + \frac{16 \hat{s} \hat{u} f_5}{(m_t^2 - \hat{u})^2} + \frac{\tilde{\kappa} f_6}{\hat{s} (m_t^2 - \hat{u}) m_W^2} \right] \quad (3)$$

where g and g_s are respectively weak and strong coupling constants and m_t , m_W are the masses of top and W gauge boson and V_{tb} is CKM matrix element. The explicit forms for f_i ($i = 1, \dots, 6$) in terms of Mandelstam variables, κ and $\tilde{\kappa}$ are given in Eqs. (7)–(12) of Appendix A.

3. Sensitivity analysis for anomalous $gt\bar{t}$ couplings

In this section, we study the total cross section of tW single top production at the LHC and study the effect of CEDM and CMDM couplings on it.

Recently, CMS Collaboration reported the measured value of cross section of tW single top production at the center-of-mass energy $\sqrt{S} = 7$ TeV with an integrated luminosity of 4.9 fb^{-1} [3]:

$$\sigma_{\text{LHC}}(pp \rightarrow tW) = 16_{-4}^{+5} \text{ [pb]}. \quad (4)$$

This measurement is in agreement with the SM expectation $15.6 \pm 0.4_{-1.2}^{+1.1}$ pb [11]. The hadronic cross section for production of tW can be obtained by integrating over the parton level cross section convoluted with the parton distribution functions:

$$\sigma(pp \rightarrow tW) = \sum_{ab} \int dx_1 dx_2 f_a(x_1, Q^2) f_b(x_2, Q^2) \hat{\sigma}(ab \rightarrow tW), \quad (5)$$

where $f_{a,b}(x_i, Q^2)$ are the parton structure functions of proton. The parameters x_1 and x_2 are the parton momentum fractions and Q is the factorization scale.

In this Letter, we obtain the direct constraints on dipole operators including top quark in the above effective Lagrangian approach. We consider the total cross section of tW single top production at the LHC and study the effect of CMDM and CEDM coupling on it. For this study, we consider the relative change in cross section which is defined as:

$$R = \frac{\Delta\sigma}{\sigma_{SM}} = \frac{\sigma - \sigma_{SM}}{\sigma_{SM}}, \quad (6)$$

where σ is total cross section in the presence of CMDM and CEDM couplings. The relative change in cross section of the single top production at the LHC is shown in Figs. 2 and 3.

In these figures, we consider that only CMDM or CEDM coupling exists and display the relative change in cross section of $\sigma(pp \rightarrow tW)$ versus κ and $\tilde{\kappa}$. In Fig. 2-a and Fig. 2-b, we have set $\sqrt{S} = 7$ TeV and $\sqrt{S} = 8$ TeV, respectively. In Fig. 2-c, as explained in the caption, we have set $\sqrt{S} = 14$ TeV which will be measured in ongoing run of the LHC. In the center of mass of energy 8 TeV and 14 TeV, NNLO SM cross section of $\sigma(pp \rightarrow tW^-)$ has been obtained 11.1 pb and 41.8 pb [11]. To calculate $\sigma(pp \rightarrow tW)$, we have used the CTEQ6.6M [13], MSTW2008 [14] and ALEKHIN2 [15] as the parton structure functions (PDF). The green curve (dashed), the pink curve (line) and blue curve (dotted) are corresponding to CTEQ6.6M, MSTW2008 and ALEKHIN2 structure functions, respectively.

An interesting observation from Figs. 2 and 3 is that the correction to tW -channel cross section due to CMDM and CEDM is sensitive to the choice of parton distribution function, in particular

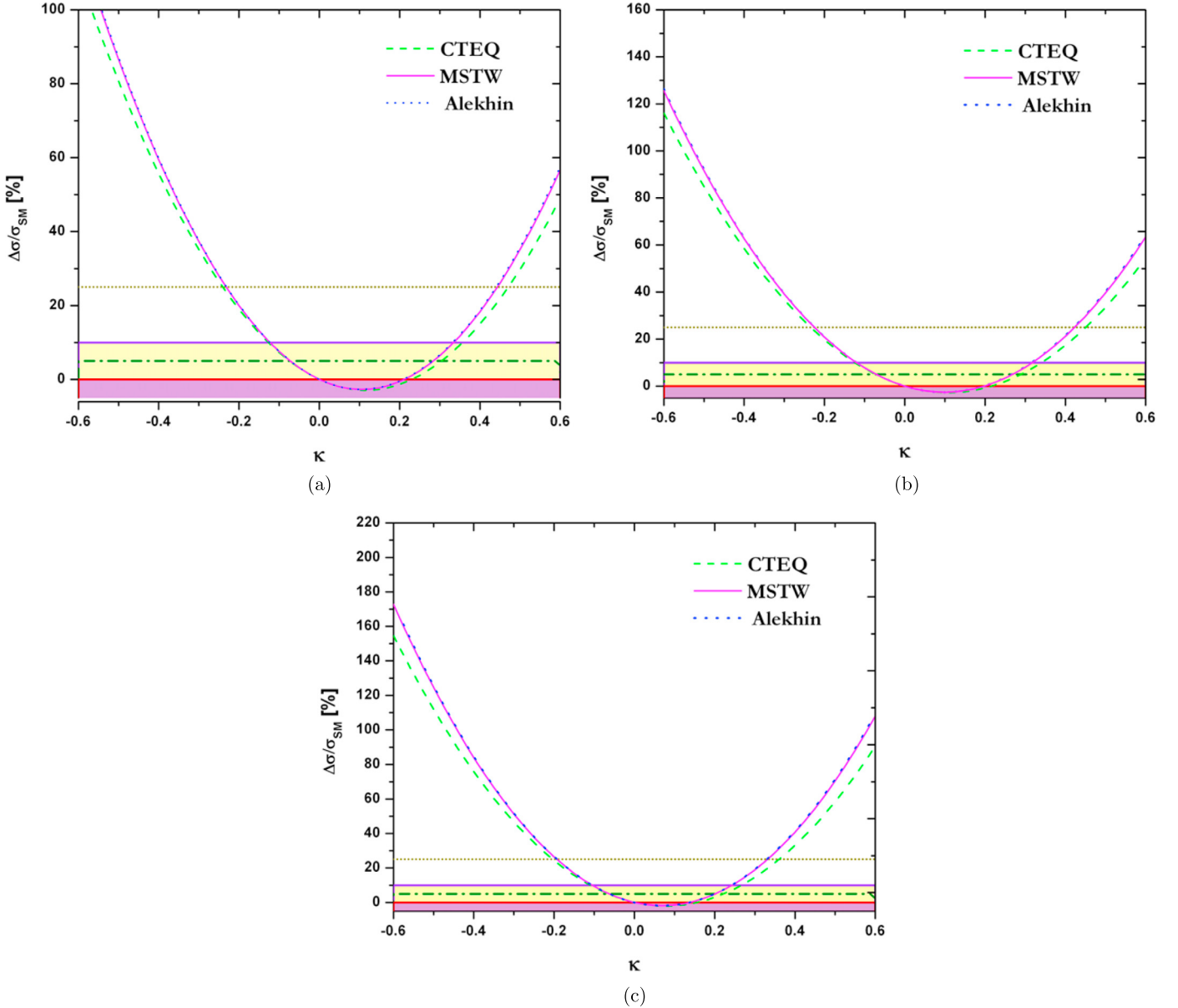


Fig. 2. (a) $\Delta\sigma(pp \rightarrow tW)/\sigma_{SM}$ versus κ . In this figure, we have set $\sqrt{s} = 7$ TeV. The green curve (dashed), the pink curve (line) and blue curve (dotted) respectively correspond to CTEQ6.6M [13], MSTW2008 [14] and ALEKHIN2 [15] structure functions. (b) and (c) are similar to (a) except that $\sqrt{s} = 8$ TeV and $\sqrt{s} = 14$ TeV, respectively. The horizontal small dotted (yellow dark), violet and dot-dashed (green) lines respectively correspond to $\pm 25\%$, $\pm 10\%$ and $\pm 5\%$ uncertainties in the measurement of $\sigma(pp \rightarrow tW)$.

at large values of κ and $\tilde{\kappa}$. As it is seen in these figures, different structure functions change the value of $\sigma(pp \rightarrow tW)$ more than 10% for large values of κ and $\tilde{\kappa}$. Considering the CTEQ PDF, the presence of κ or $\tilde{\kappa}$ can change total cross section more than 10 pb. At small value in the range of $[-0.2, 0.2]$, $\Delta\sigma(pp \rightarrow tW)/\sigma_{SM}$ is almost robust against the choice of PDF.

Fig. 2 demonstrates that the effect of the presence of CMDM can change the total cross section more than 40% for $\kappa = 0.4$. The horizontal small dotted (yellow dark), violet and dot-dashed (green) lines respectively correspond to $\pm 25\%$, $\pm 10\%$ and $\pm 5\%$ uncertainties in the measurement of $\sigma(pp \rightarrow tW)$. As it was mentioned, the total statistical and systematic uncertainties in the measurement of cross section for tW single top production at the LHC is about 25% with an integrated luminosity of 4.9 fb^{-1} at center-of-mass energy of 7 TeV. With 10% uncertainty in future measurement of the total cross section, from Fig. 2 (Fig. 3), we can put upper bound on κ ($\tilde{\kappa}$) down to 0.14 (0.23). If in forthcoming

run of LHC (in 14 TeV), we measure the total cross section even with 5% uncertainty, we can constrain κ ($\tilde{\kappa}$) down to 0.07 (0.14). As it is seen in Fig. 3, in spite of CMDM (κ), the cross section is symmetric with respect to $\tilde{\kappa}$ because CEDM coupling enters in the cross section in even powers when $\kappa = 0$. Therefore, in this situation, the cross section is not a CP-violating observable.

Another observation from Fig. 2 is that the effect of presence of CMDM (κ), in spite of CEDM ($\tilde{\kappa}$), can be destructive. If the total uncertainty in the measurement of cross section is less than 5%, we can distinguish between CEDM and CMDM effects.

In Fig. 4, red area depicts ranges of parameters space in CMDM (κ) and CEDM ($\tilde{\kappa}$) couplings plane for which prediction of effective Lagrangian (Eq. 1) on tW single top production at LHC is consistent with experimental measurements. When performing such study, one should take into account constraints from other studies. There exist many direct and indirect constraints on dipole operators. Presently, the most sensitive observable obtained from

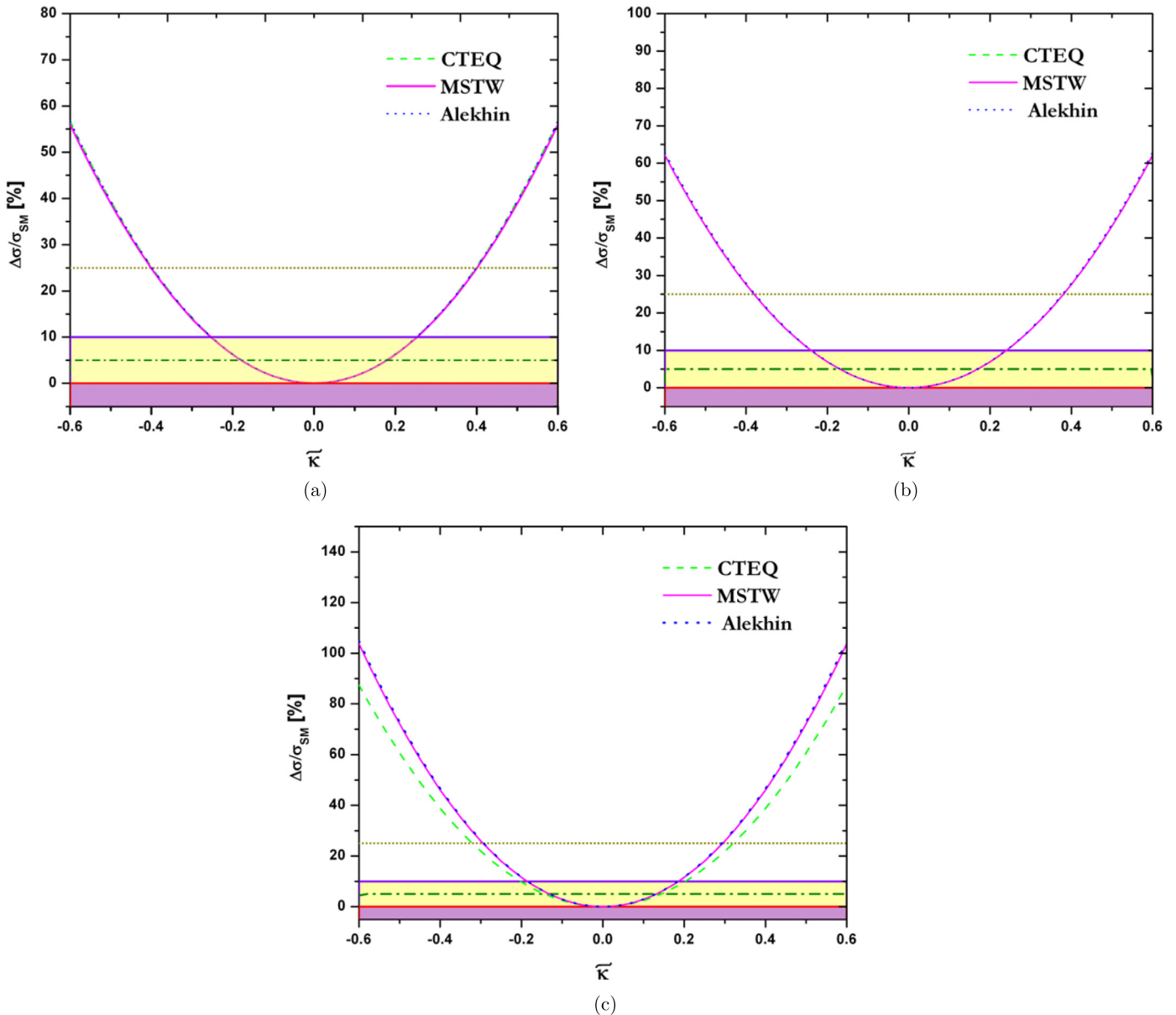


Fig. 3. (a) $\Delta\sigma(pp \rightarrow tW)/\sigma_{SM}$ versus $\tilde{\kappa}$ for the center-of-mass energy of 7 TeV (left), 8 TeV (right) and 14 TeV in bottom. Input parameters are similar to Fig. 2.

mercury and neutron EDMs. In [6], it is shown that the neutron EDM constrains the top CEDM to be $\tilde{\kappa} < 8 \times 10^{-3}$. Moreover, the constraints from d_{Hg} and the top electric dipole moment, provide weaker bound on $\tilde{\kappa}$. Furthermore, the CEDM and CMDM couplings of the top quark directly affect on top pair production at hadron colliders [12]. We have borrowed the results of LHC constraints which come from $t\bar{t}$ total cross section on CEDM and CMDM of top from Ref. [6]. These results have been shown in Fig. 4. In this figure green line depicts neutron EDM constraint on $\tilde{\kappa}$. Hatched cyan shaded area depicts the allowed region which is consistent with $t\bar{t}$ total cross section at LHC. Yellow area shows the allowed region which is consistent with spectrum measurement of $m_{t\bar{t}}$ at LHC. It is remarkable that the allowed regions of top pair production cross section and spectrum measurement of $m_{t\bar{t}}$ at the LHC overlap with allowed region of tW single top production at LHC. As it can be seen in this figure, tW single top constraints on κ and $\tilde{\kappa}$ are stronger than direct constraints which come from $t\bar{t}$ total cross section and spectrum measurement of $m_{t\bar{t}}$ at LHC.

In study of the top quark, the top quark spin observables have been found to be useful and sensitive to several models beyond the SM. In [16–18], it was shown that the $t\bar{t}$ spin correlation and spin related asymmetries in decay product of the top quarks are sensitive to CEDM and CMDM. In [16], it has been shown that with present experimental precision on measurement of the top spin observables, the CEDM and CMDM can be determined with an uncertainty of a few percent.

4. Concluding remarks

In this Letter, based on the effective Lagrangian approach, we modify the SM by the additional 5-dimensional operators which include the interaction of top quark with gluon and consider the effect of this Lagrangian in production of tW single top. Coefficients of this Lagrangian are related to CEDM and CMDM form factors. We consider the total cross section of tW single top production at the LHC and study the effect of CEDM and CMDM

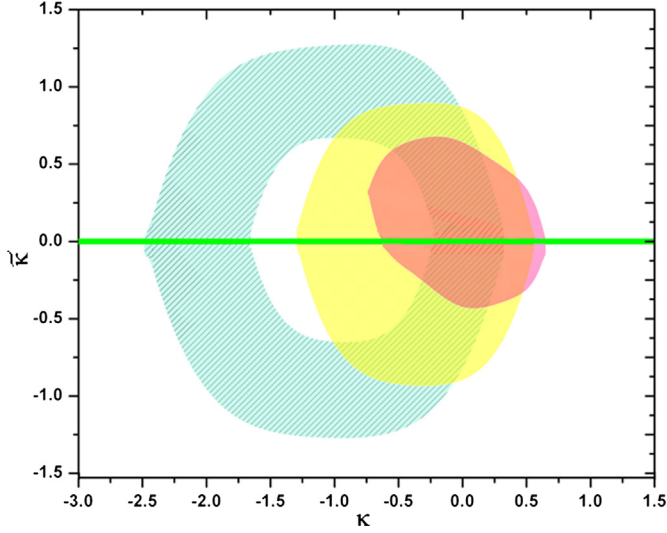


Fig. 4. Red area depicts ranges of parameters space in CMDM (κ) and CEDM ($\tilde{\kappa}$) couplings plane for which prediction of gluonic dipole effective Lagrangian on tW single top production at LHC is consistent with experimental measurements. Green line shows neutron EDM constraint on $\tilde{\kappa}$. Hatched cyan (yellow) shaded area depicts the allowed region which is consistent with $t\bar{t}$ total cross section (spectrum measurement of $m_{t\bar{t}}$) at LHC. Shaded area which depict $t\bar{t}$ -channel constraints have been borrowed from [6]. (For interpretation of the references to color, the reader is referred to the web version of this article.)

couplings on it. We have found the allowed regions in parameters space of CEDM and CMDM in such a way that the experimental measurement of $\sigma(pp \rightarrow tW)$ is satisfied. We also investigate the effect of different PDFs on tW single top production at LHC as a function of κ and $\tilde{\kappa}$.

We have shown that deviation of the tW -channel single top cross section from the SM value is significant. We consider constraints on CEDM and CMDM couplings which come from $t\bar{t}$ total cross section and spectrum measurement of $m_{t\bar{t}}$ at the LHC and compare them with our results. We have shown that constraints on κ and $\tilde{\kappa}$ which arise from tW single top production at LHC are comparable with the ones coming from $t\bar{t}$ production at the LHC. It is notable that with the current tW cross section precision measurement, tight bounds are obtained and therefore with more precision measurements in future even more stringent limits than $t\bar{t}$ cross section could be achieved.

Acknowledgement

We would like to thank H. Kanpour for helping us in technical issues.

Appendix A

Here, we list the formulas of f_i which have been applied in calculation of single top production cross section. Notice that mass dimensions of f_i are not equal.

$$f_1 = 16\hat{s}m_t^2 - 16\kappa\hat{s}m_t^2 + 20\kappa^2\hat{s}m_t^2 - 16\hat{u}m_t^2 + 24\kappa^2\hat{u}m_t^2 - 10\kappa^2m_t^4 - 16\hat{u}m_t^4 + 24\kappa m_t^4 + 32\hat{u}^2m_t^2, \quad (7)$$

$$f_2 = (-4\hat{s}\kappa^2 - 32\hat{s}\kappa + 16\hat{u})m_t^8 + \hat{u}((16\kappa^2 + 96\kappa + 32)\hat{s} + 48\hat{u})m_t^6 + \hat{u}^2((-24\kappa^2 - 96\kappa - 64)\hat{s} - 80\hat{u})m_t^4$$

$$+ \hat{u}^3((16\kappa^2 + 32\kappa + 32)\hat{s} + 32\hat{u})m_t^2 - 4\kappa^2\hat{s}\hat{u}^4 - 16m_t^{10}, \quad (8)$$

$$f_3 = 8m_t^{10} + (-16\hat{s} - 8\hat{u})m_t^8 + (8\hat{s}^2 + (10\kappa^2 - 16\kappa + 16)\hat{u}\hat{s} + 8\hat{u}^2)m_t^6 + \hat{u}((-10\kappa^2 + 16\kappa - 8)\hat{s}^2 - 8\hat{u}^2 + (-20\kappa^2 + 16\kappa - 16)\hat{s}\hat{u})m_t^4 + (12\hat{s} + 10\hat{u})\kappa\hat{s}\kappa\hat{u}^2m_t^2 - 2\kappa^2\hat{s}^2\hat{u}^3, \quad (9)$$

$$f_4 = -4m_W^4 + (4\hat{s} + 4\hat{u})m_W^2 - 2\hat{s}\hat{u} + m_t^2(2\hat{u} - 2m_W^2), \quad (10)$$

$$f_5 = -16\hat{s}\hat{u} - 16\kappa\hat{s}\hat{u} - 24\kappa^2\hat{s}\hat{u} - 24\kappa\hat{u}^2 - 18\kappa^2\hat{u}^2 - \frac{16\hat{u}^3}{\hat{s}} + \frac{4\kappa^2\hat{s}\hat{u}^2}{m_t^2} + \frac{4\kappa^2\hat{u}^3}{m_t^2}, \quad (11)$$

$$f_6 = \kappa\hat{s}[(8\hat{u} - 8m_W^2)m_t^2 + \hat{u}(-8\hat{s} - 8\hat{u}) + (16\hat{s} + 8\hat{u})m_W^2] \quad (12)$$

where s , t and u are Mandelstam variables, m_t , m_W are the masses of top and W gauge boson. The parameters $\tilde{\kappa}$ and κ are, respectively CEDM and CMDM couplings.

References

- [1] F.-P. Schilling, *Int. J. Mod. Phys. A* 27 (2012) 1230016, arXiv:1206.4484 [hep-ex].
- [2] W. Buchmuller, D. Wyler, *Nucl. Phys. B* 268 (1986) 621; C. Arzt, M.B. Einhorn, J. Wudka, *Nucl. Phys. B* 433 (1995) 41, arXiv:hep-ph/9405214; G.J. Gounaris, M. Kuroda, F.M. Renard, *Phys. Rev. D* 54 (1996) 6861, arXiv:hep-ph/9606435; A. Cordero-Cid, M.A. Perez, G. Tavares-Velasco, J.J. Toscano, *Phys. Rev. D* 70 (2004) 074003, arXiv:hep-ph/0407127; B. Grzadkowski, Z. Hioki, K. Ohkuma, J. Wudka, *Nucl. Phys. B* 689 (2004) 108, arXiv:hep-ph/0310159; B. Grzadkowski, M. Iskrzynski, M. Misiak, J. Rosiek, *J. High Energy Phys.* 1010 (2010) 085, arXiv:1008.4884 [hep-ph]; R. Torre, arXiv:1005.4801 [hep-ph].
- [3] S. Chatrchyan, et al., CMS Collaboration, *Phys. Rev. Lett.* 110 (2013) 022003, arXiv:1209.3489 [hep-ex].
- [4] E.O. Iltan, *Phys. Rev. D* 65 (2002) 073013, arXiv:hep-ph/0111038.
- [5] R. Martinez, M.A. Perez, N. Poveda, *Eur. Phys. J. C* 53 (2008) 221, arXiv:hep-ph/0701098.
- [6] J.F. Kamenik, M. Papucci, A. Weiler, *Phys. Rev. D* 85 (2012) 071501, arXiv:1107.3143 [hep-ph].
- [7] Z. Hioki, K. Ohkuma, *Phys. Rev. D* 88 (2013) 017503, arXiv:1306.5387 [hep-ph]; Z. Hioki, K. Ohkuma, *Phys. Lett. B* 716 (2012) 310, arXiv:1206.2413 [hep-ph].
- [8] T. Ibrahim, P. Nath, *Phys. Rev. D* 84 (2011) 015003, arXiv:1104.3851 [hep-ph]; T. Ibrahim, P. Nath, *Phys. Rev. D* 82 (2010) 055001, arXiv:1007.0432 [hep-ph].
- [9] T.G. Rizzo, *Phys. Rev. D* 50 (1994) 4478, arXiv:hep-ph/9405391.
- [10] J.L. Hewett, T.G. Rizzo, *Phys. Rev. D* 49 (1994) 319, arXiv:hep-ph/9305223.
- [11] N. Kidonakis, arXiv:1205.3453 [hep-ph].
- [12] D. Atwood, A. Kagan, T.G. Rizzo, *Phys. Rev. D* 52 (1995) 6264, arXiv:hep-ph/9407408; P. Haberl, O. Nachtmann, A. Wilch, *Phys. Rev. D* 53 (1996) 4875, arXiv:hep-ph/9505409; C. Degrande, J.-M. Gerard, C. Grojean, F. Maltoni, G. Servant, *J. High Energy Phys.* 1103 (2011) 125, arXiv:1010.6304 [hep-ph]; Z. Hioki, K. Ohkuma, *Eur. Phys. J. C* 65 (2010) 127, arXiv:0910.3049 [hep-ph]; Z. Hioki, K. Ohkuma, *Eur. Phys. J. C* 71 (2011) 1535, arXiv:1011.2655 [hep-ph]; S.S. Biswal, S.D. Rindani, P. Sharma, arXiv:1211.4075 [hep-ph].
- [13] J. Pumplin, D.R. Stump, J. Huston, H.L. Lai, P.M. Nadolsky, W.K. Tung, *J. High Energy Phys.* 0207 (2002) 012, arXiv:hep-ph/0201195.
- [14] A.D. Martin, W.J. Stirling, R.S. Thorne, G. Watt, *Eur. Phys. J. C* 63 (2009) 189, arXiv:0901.0002 [hep-ph].
- [15] S. Alekhin, J. Blumlein, S. Klein, S. Moch, arXiv:0908.3128 [hep-ph].
- [16] W. Bernreuther, Z.-G. Si, arXiv:1305.2066 [hep-ph].
- [17] M. Baumgart, B. Tweedie, *J. High Energy Phys.* 1303 (2013) 117, arXiv:1212.4888 [hep-ph].
- [18] K.-m. Cheung, *Phys. Rev. D* 55 (1997) 4430, arXiv:hep-ph/9610368.